

# LOCAL INSTABILITIES OF ALFVÉN WAVES IN HIGH SPEED STREAMS

B. BAVASSANO, M. DOBROWOLNY, and G. MORENO

*Laboratorio per il Plasma nello Spazio, CNR, Via G. Galilei, C.P. 27, 00044 Frascati, Italy*

(Received 13 June, 1977; in revised form 17 January, 1978)

**Abstract.** A two fluid stability analysis of an inhomogeneous solar wind plasma leads to prediction of possible instabilities of both Alfvénic and magnetoacoustic waves driven by local velocity gradients. The waves predicted to be possibly unstable have short wavelengths in comparison with the length scale of the gradients and, with different thresholds for the value of velocity shear, may have different directions of propagation with respect to the background magnetic field.

We have performed a detailed study, based on Pioneer 6 magnetic and plasma data relative to several high speed streams in the solar wind, on the direction of propagation of the transverse waves which are found within the streams and on their association with velocity gradients within the stream structure. The analysis leads to the conclusion that the observed Alfvén waves may be consistent with the hypothesis of local generation through one of the above mentioned instabilities where velocity shear leads in fact to excitation of incompressible waves in directions almost parallel to the magnetic field.

## 1. Introduction

Observational evidence of large amplitude Alfvén waves in the interplanetary medium has been reported from several experiments (Belcher and Davis, 1969, 1971; Martin *et al.*, 1973; Daily, 1973; Burlaga and Turner, 1976).

Some main points which result from the different investigations are the following: (1) Alfvén waves seem to dominate the microscale structure with respect to magnetosonic disturbances which are never observed as clearly, (2) such Alfvén waves are mostly propagating outwardly from the Sun with a clear tendency to be almost parallel to the magnetic field direction, (3) they are particularly evident within the trailing edges of the high speed streams (where velocity decreases with time). On the other hand, the leading edges (or compression regions of the streams) show a much more complicated structure which is claimed to contain both Alfvénic and magnetosonic fluctuations with direction of propagation also towards the Sun (Belcher and Davis, 1971).

Concerning the origin of the observed Alfvén waves, one hypothesis which is advanced is that of generation at the Sun. More specifically (see Hollweg, 1975) both magnetoacoustic and Alfvénic modes would be generated through photospheric supergranulation. The magnetoacoustic modes would be quickly Landau damped. On the other hand, linearly polarized Alfvén waves would damp non linearly inside about 0.5 AU but then would be converted into circularly polarized Alfvén waves, which do not undergo Landau damping and are therefore observed at 1 AU (Barnes and Hollweg, 1974). A good point in favour of this interpretation of the observed waves is that, as long as the waves are produced at distances from

the Sun less than the Alfvénic critical point, only those propagating away from the Sun will be possibly observed in the superalfvénic solar wind (Belcher and Davis, 1971). Thus the hypothesis of generation at the Sun gives an explanation for the preferential direction of propagation of the observed waves at 1 AU.

According to this point of view, the experimental fact that the waves are preferentially observed in connection with high velocity streams is attributed to the fact that the streams themselves are driven by the waves (Hollweg, 1973, 1975). The further observational fact that the largest amplitude Alfvénic fluctuations are found in the compression region at the leading edges of the high velocity streams (Belcher and Davis, 1971), is then related to the larger average magnetic field in such regions, with respect to that in the trailing edges of the streams.

A second alternative on the origin of the observed Alfvén waves is that of local generation, i.e. generation through some local instabilities.

Among possible candidates, velocity shear instabilities are suggested by the association of the observed waves with high velocity streams. Another possibility of local generation would be the presence of non thermal features of the particle distributions. Although non thermal ion distributions have been found to be sometimes associated with high speed streams (Feldman *et al.*, 1974) (in particular double-peaked proton distributions), the association is not as general as the association of the Alfvén waves with the streams. Furthermore, from theoretical analysis (Gary *et al.*, 1975; Abraham-Shrauner and Feldman, 1977) it is found that double peaked distributions should lead mainly to ion cyclotron waves having frequencies of a few hertz in the plasma frame (and wavelengths of the order of the ion Larmor radius) whereas the spectrum of all the Alfvén waves observed in the wind extends to much lower frequencies and correspondingly larger wavelengths, up to  $5 \times 10^6$  km (Belcher and Davis, 1971).

Thus it is plausible to say that, even if kinetic mechanisms are operating at times, they certainly do not account for all the Alfvén waves observed.

Quite apart from the particular instability that one is considering, it must be remarked here that testing with the data an hypothesis of local generation implies a local or quasi-local analysis of the data, in that the local properties of the plasma (as, for example, the gradients) and the local properties of the waves must be correlated with a given instability theory.

No analysis of this type has been done so far as all the previous investigations had a statistical character, referring to periods of several days and even to several streams.

In the present paper we propose to test magnetic and plasma data relative to some high speed streams (and therefore containing Alfvén waves) against the hypothesis of local generation of these waves through velocity shear instabilities. In particular, we will compare the analysis with some recent theories of velocity shear instabilities in high  $\beta$  plasmas (Dobrowolny, 1972, 1977), predicting the possibility of generation of magnetohydrodynamic waves of small wavelengths in comparison with the typical length scale of the gradients.

The plan of the paper is the following: in Section 2 we summarize the results of theories of velocity shear instabilities in high  $\beta$  plasma giving the stability criteria for different types of excitations. Section 3 describes the minimum variance analysis applied to magnetic field data, within two high velocity streams, to investigate the properties of the observed waves. A general discussion on the properties of waves associated with streams is given in Section 4. Section 5 compares some results of the analysis with the criteria for various velocity shear instabilities. It appears that the data are consistent with the occurrence of one instability of Alfvén waves with propagation almost parallel to the magnetic field direction. On the other hand it is also demonstrated that the local velocity gradients are not sufficient for excitation of magnetosonic modes and of Alfvén waves propagating in a direction quasi perpendicular to the magnetic field.

This does not lead to the conclusion of a mechanism for Alfvén wave generation alternative to that of generation at the Sun. Rather, it is shown that one instability driven by velocity shear may be relevant in exciting part of the waves observed in the high-velocity streams. The favorable indications in this direction along with the critical points of a theory of velocity shear generation are discussed at length in Section 5. Section 6 contains further criticism and the conclusions.

## 2. Velocity Shear Instabilities in a High $\beta$ Plasma

We refer in the following to instabilities driven by velocity shear in a plasma with a uniform magnetic field  $\mathbf{B}_0$  and a velocity flow  $\mathbf{v}_0$  parallel to the magnetic field and inhomogeneous in a perpendicular direction. Referring to the solar wind, one obtains the condition of flow parallel to the magnetic field in a corotating reference frame: thus, in this frame, the model, although simplified, can be used to represent the high speed streams.

The ordinary Kelvin Helmholtz instability (Chandrasekhar, 1961) is obtained, as it is well known, by simulating the velocity gradient with a discontinuous jump and therefore refers to waves with wavelengths larger than the scale length  $L$  of the velocity profile, i.e.

$$kL < 1, \quad (1)$$

$k$  being the wave vector of the waves. For instability one finds the condition

$$\Delta v_0 \geq v_A, \quad (2)$$

where  $\Delta v_0$  is the velocity jump and  $v_A$  the Alfvén speed. The wavelength condition (1), however, excludes this instability from being of interest for the waves observed in the streams as their spectrum contains wavelengths up to 0.05 AU (Belcher and Davis, 1971) while the typical scale length of the large velocity variation in a stream is  $L \sim (0.1-0.3)$  AU.

Very recently a numerical solution of the Kelvin Helmholtz problem has been given using continuous velocity (and density) profiles (Dobrowolny and Paravano,

1977). The main result which must be recalled here is that the unstable waves are still, roughly, characterized by condition (1), i.e. no instability is essentially found for wavelengths much smaller than  $L$ . This rules out completely the ordinary Kelvin Helmholtz instability as an explanation for the Alfvén waves observed in streams.

Further theoretical work has been done (Dobrowolny, 1972, 1977) on the possibility of having velocity shear instabilities for small wavelengths, i.e. for

$$kL > 1. \quad (3)$$

This work, of which we recall here the main results, is based on a two fluid description of the plasma including finite Larmor radius effects of the plasma ions (therefore a non-magnetohydrodynamic description). It refers to waves of frequencies  $\omega$  smaller than the proton gyrofrequency  $\Omega_{ci}$  and wavelengths larger than the ion Larmor radius  $a_i$ , i.e.

$$\omega \ll \Omega_{ci}, \quad ka_i \ll 1. \quad (4)$$

The waves have a component of propagation along the magnetic field such that the corresponding phase velocity is intermediate between ion ( $v_{thi}$ ) and electron ( $v_{the}$ ) thermal velocities,

$$v_{thi} < \frac{\omega}{k_{\parallel}} < v_{the}, \quad (5)$$

where  $k_{\parallel}$  is the wave vector component parallel to the magnetic field. Finally, the theory is done in WKB approximation, consistently with condition (3) and is general with respect to the plasma  $\beta$  ( $\beta = 4\pi n_0(T_e + T_i)/B_0^2$  being the ratio of particle pressure to magnetic pressure).

Notice that condition (5) is still consistent with values of  $\beta$  of order unity, like in a typical solar wind at 1 AU, as the frequency in (5) is that in the laboratory frame, and, for the case of flowing plasmas, one finds typical values of the order of the Alfvén speed or the sound speed for the wave phase velocity  $\Omega/k_{\parallel}$  constructed with the Doppler shifted frequency  $\Omega = \omega - k_{\parallel}v_0$ .

The instabilities which are found are due to finite Larmor effects of the ions (or collisionless ion viscosity) and are therefore essentially different from the ordinary magnetohydrodynamic instability.

More specifically it is found that magnetosonic waves are driven unstable only for directions of propagation quasi perpendicular to the background magnetic field, i.e. for

$$\frac{k_{\perp}}{k_{\parallel}} \gg 1. \quad (6)$$

Here  $k_{\perp}$  is the wave vector component perpendicular to both the background magnetic field  $\mathbf{B}_0$  and the direction of the velocity (and density) gradients. Hence, with reference to solar ecliptic coordinates and an ideal Parker's model of the solar

wind,  $k_{\perp}$  is the component of  $\mathbf{k}$  along the normal  $\mathbf{N}$  to equatorial plane. Notice also that, because of conditions (5),  $k_{\parallel}$  must be different from zero.

The following dispersion relation is derived (Dobrowolny, 1972) under condition (6) and for magnetosonic waves:

$$\Omega_i = \frac{1}{2} \left\{ -\omega_i^* \left( 1 + \frac{T_e}{T_i} \right) \pm \left[ \left( 1 + \frac{T_e}{T_i} \right)^2 \omega_i^{*2} + \frac{4}{1+\beta} k_{\parallel}^2 c_s^2 \left( 1 - \frac{k_{\perp}}{k_{\parallel}} \xi \right) \right]^{1/2} \right\}. \quad (7)$$

In Equation (7)

$$\omega_i^* = k_{\perp} v_{\text{thi}} \frac{a_i}{L_N}$$

is the ion drift frequency, with  $L_N$  the scale length of the density profile;  $\Omega_i$  is the Doppler shifted frequency

$$\Omega_i = \omega - k_{\parallel} v_0 - \omega_i^* \quad (8)$$

and  $c_s^2 = (T_e + T_i)/m_i$  is the sound speed. Finally, we have introduced the shear parameter

$$\xi = \frac{v'_0}{\Omega_{ci}}, \quad (9)$$

where  $v'_0$  is the derivative of the velocity flow (in the azimuthal direction) and  $\Omega_{ci} = |e| B_0/m_i c$  is the ion cyclotron frequency. Correspondingly, the instability conditions are

$$\begin{aligned} \frac{k_{\perp}}{k_{\parallel}} \xi &> 0, \\ \frac{k_{\perp}}{k_{\parallel}} \xi &> 1 + \frac{1}{4} \left( 1 + \frac{T_e}{T_i} \right) (1 + \beta) \frac{k_{\perp}^2}{k_{\parallel}^2} \frac{a_i^2}{L_N^2}. \end{aligned} \quad (10)$$

As it is seen, the density gradient exerts a stabilizing effect.

Alfvén waves are found to be possibly unstable for directions of propagation within two small cones around the directions both perpendicular and parallel to the magnetic field. For quasi-perpendicular propagation, i.e. under condition (6), the wave dispersion relation is (Dobrowolny, 1972)

$$\Omega_i = \frac{1}{2} \left\{ -\frac{1}{2}(1 + \beta)\omega_i^* \pm \left[ \frac{1}{4}(1 + \beta)^2 \omega_i^{*2} + 4k_{\parallel}^2 v_A^2 \left( 1 + \frac{1}{2}\beta_i \frac{k_{\perp}}{k_{\parallel}} \xi \right) \right]^{1/2} \right\}, \quad (11)$$

where  $\beta_i = 4\pi n_0 T_i/B_0^2$  and the corresponding instability conditions are

$$\begin{aligned} \frac{k_{\perp}}{k_{\parallel}} \xi &< 0, \\ \left| \frac{k_{\perp}}{k_{\parallel}} \xi \right| &> \frac{2}{\beta_i} \left[ 1 + \frac{1}{16}(1 + \beta)^2 \beta_i \frac{k_{\perp}^2}{k_{\parallel}^2} \frac{a_i^2}{L_N^2} \right]. \end{aligned} \quad (12)$$

Notice that for small density variations (as in trailing edges of the high velocity streams), one has  $\omega_i^*$  very small and from (7) and (10) it is found that  $\text{Re } \Omega_i$  tends to zero ( $\Omega_i$  being the frequency in the plasma frame). In such cases (i.e. the limit  $L_N \rightarrow \infty$ ), the real part of the frequency  $\omega$  (the frequency in the laboratory frame), is simply equal to the Doppler shift  $k_{\parallel}v_0$  and conditions (4) and (5) are still verified for the supersonic wind.

For quasi-parallel propagation, i.e. for

$$\frac{k_{\parallel}}{k_{\perp}} \gg 1, \quad (13)$$

the dispersion relation reads

$$\frac{\Omega_{\pm}^2}{k_{\parallel}^2 V_A^2} = (1 - \frac{3}{2}\eta) \pm \frac{1}{2}\sqrt{\eta(9\eta - 8)} \quad (14)$$

having introduced the parameter

$$\eta = \beta_i \frac{k_{\parallel}}{k_{\perp}} \xi. \quad (15)$$

In (14)  $\Omega = \omega - k_{\parallel}v_0$  is the wave frequency shifted by the Doppler effect due to the plasma flow and the signs  $\pm$  indicate that the usual Alfvén branch is split into two by the effect of velocity shear ( $\eta \neq 0$ ). Notice that density gradients do not appear in the solution (14) as the corresponding drift frequency terms (perpendicular drifts) enter only in the limit (6) of mainly perpendicular propagation (Kadomtsev, 1965). The instability condition corresponding to (14) is simply (Dobrowolny, 1977)

$$\eta > 0. \quad (16)$$

Upon increasing  $\eta$ , as seen from (14), both branches  $\Omega_{\pm}^2$  are seen to give both damped and unstable roots, with the same real and imaginary parts of the frequency (in absolute values) for  $\eta$  in the range  $0 < \eta < \frac{8}{9}$ . The maximum growth rate in this range is

$$\gamma_{\max} \sim 0.54 k_{\parallel} V_A, \quad (17)$$

obtained for  $\eta = \frac{2}{3}$ . The growth rate of the two branches becomes then different for  $\eta > \frac{8}{9}$  (Dobrowolny, 1977). With reference to the solar wind data, however, as will be seen in Section 5, it is  $\eta < 1$  and small values of  $\eta$  that are of most interest.

Notice that condition (16) shows that instability (when  $\beta_i \sim 1$ ) is obtained starting from small values of  $(k_{\parallel}/k_{\perp})\xi$ . Comparing with the conditions (10) and (12) for quasi-perpendicular instabilities, requiring  $(k_{\perp}/k_{\parallel})\xi > 1$ , it is therefore seen that one has a larger cone of unstable Alfvén waves propagating around the magnetic field direction, than the cones of unstable Alfvén or magnetosonic waves around the perpendicular direction.

### 3. Data Reduction

The present study has been based on plasma and magnetic field data collected simultaneously by the spacecraft Pioneer 6 within two high velocity streams occurring in January and February 1966. The instrumental apparatus of the plasma and magnetic field experiments on board of Pioneer 6 has been described elsewhere (Ness *et al.*, 1966; Ness, 1970; Lazarus *et al.*, 1973) and will not be recalled here.

Our analysis has been restricted to periods of time (from Day 34, 4:00 UT to Day 36, 4:00 UT and from Day 50, 0:00 UT to Day 54, 4:00 UT) during which relatively strong velocity gradients were observed. Figure 1, given as a reference, shows hourly averages of a high velocity stream from day 50 to 53. For the remaining periods investigated see plots of hourly averages given by Lazarus *et al.* (1973).

Single (71 s) plasma data were made available to us by Dr A. Lazarus of the Massachusetts Institute of Technology; magnetic field data, in the form of 30 s averages of the field components, were supplied by the World Data Center (Washington).

To determine the direction of the wave propagation vector  $\mathbf{k}$ , a variance matrix analysis has been used on the 30-s magnetic field averages. The variance matrix is defined as:

$$T_{ij} = \langle B_i B_j \rangle - \langle B_i \rangle \langle B_j \rangle,$$

where  $B_i, B_j$  ( $i, j = 1, 2, 3$ ) are cartesian components of the magnetic field vector ( $\mathbf{B}$ ). In the case of a large amplitude Alfvén wave, this matrix will have a well defined direction of minimum variance ( $\mathbf{M}_1$ ) parallel (or antiparallel) to  $\mathbf{k}$ .

The minimum variance analysis has been performed over 20 min periods.

This period allows to have a meaningful number of data (40) within each interval and, on the other hand, is sufficiently short for having a quasi local determination of plasma and wave properties not affected by large variations on longer time scales.

No filtering on the data, in the way used by Daily (1973), has been employed. Filtering could indeed be motivated by the necessity of excluding, from the variance matrix, power from large scale inhomogeneities of the field, thus remaining with power from Alfvénic fluctuations only (in Daily's work the effective bandwidth entering the variance matrix is from 0.03 Hz to 0.003 Hz). However a careful analysis of the filtering procedure used by Daily (Jenkins and Watts, 1969) reveals that it introduces a most heavy bias into the variance analysis. Figure 2 illustrates its effects on the magnitude of the magnetic field. A 20 min period where  $|\mathbf{B}|$  is approximately constant (line labelled *A* in the Figure) has been considered. Application of the Daily's filtering procedure to each component of the magnetic field, produces the behaviour of  $|\mathbf{B}|$  shown by the line labelled *B* in the figure and containing large spurious fluctuations. Looking at such filtered data, one could argue, erroneously, that the fluctuations are not Alfvénic.

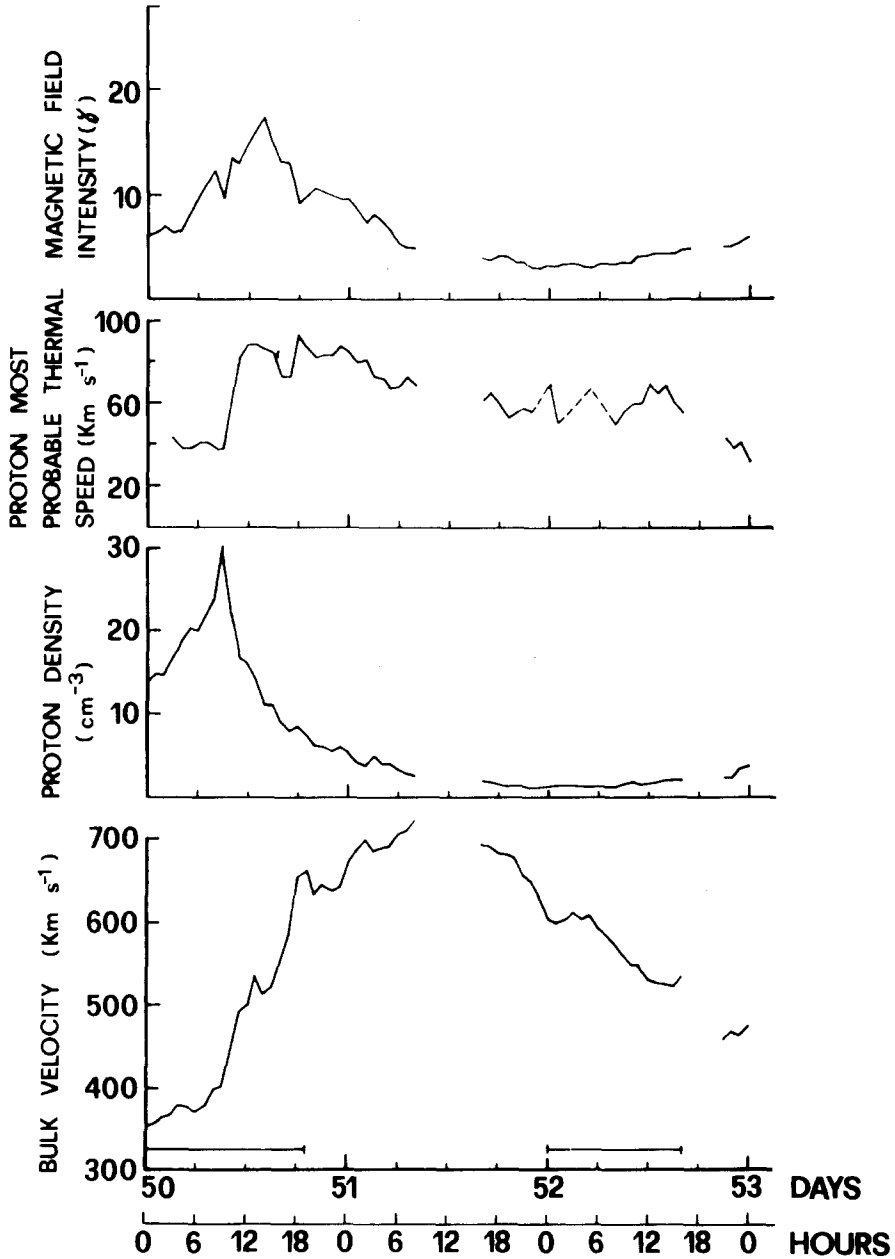


Fig. 1. Time history of solar wind parameters during the high-velocity stream observed by Pioneer 6 from 19 February to 23 February, 1966. The horizontal bars at the bottom of the figure indicate the periods of time illustrated in Figure 3.



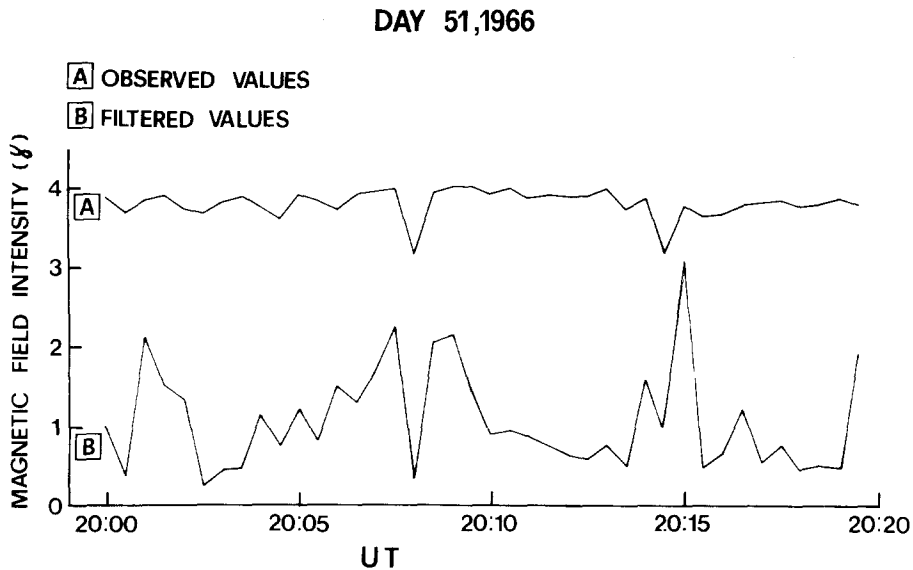


Fig. 2. Effects of the filtering procedure on the interplanetary magnetic field intensity. The line labelled A gives the observed intensity; the one labelled B gives the intensity, when the filtering procedure is applied to each component of the magnetic field (see text for details).

A further comparison with Daily's minimum variance work is obtained by evaluating the number of 20 min blocks of data which do not meet the following criteria (adopted by Daily in his analysis): (1) the eigenvalues of the variance matrix should verify  $\lambda_3/\lambda_2 \leq 0.50$  and  $\lambda_2/\lambda_1 \leq 0.55$ , to have sufficiently well defined directions of minimum and maximum variance; (2) the largest eigenvalue  $\lambda_1$  must be at least 6 times the variance of the field magnitude  $\sigma_B^2$  (in order to discriminate against non Alfvénic fluctuations).

Out of the total number of 20 min blocks of data considered in the present study (407), 72 (18%) did not satisfy the constraint (1); 29 (7%) the constraint (2).

According to Daily (who examined Pioneer 6 data from day 26 to day 40), 29% of the data samples did not meet the first constraint and 44% the second. The very large difference between his and our analysis, occurring for the second criterion, corresponds to the bias effect of the filtering procedure illustrated in Figure 2. On the other hand, even the percentage of data not satisfying the first criterion is significantly larger when the filtering procedure is applied.

A further minor difference between the present analysis and that accomplished by Daily consists in the procedure used to select data. In fact, while leaving the constraint (2) unmodified, we have changed the constraint (1), by rejecting only data blocks with  $\lambda_3/\lambda_2 \leq 0.50$ . The reason is that a well defined direction of minimum variance is obtained even when the two largest eigenvalues are comparable [ $(\lambda_2/\lambda_1) \geq 0.55$ ]:  $\lambda_2 \approx \lambda_1$  is expected, indeed, in the case of circularly polarized Alfvén waves, which should not be discarded from the analysis. It is found,

however, that retaining data with  $\lambda_2/\lambda_1 \geq 0.55$  produces only a slight variation in the percentage of rejected data blocks. In all, the following study will be based on 331 20-min blocks of data.

Some results of our minimum variance analysis are shown in Figures 3a and 3b which refer to day 50 and 52 corresponding respectively to leading and trailing edges of the high speed stream of Figure 1. Here we have plotted the ratios  $\lambda_3/\lambda_2$ ,  $\lambda_2/\lambda_1$ ,  $\sigma_B^2/\lambda_1$  and, on the top panel, the direction of minimum variance of the magnetic field which, in the case of wave identification, coincides with the wave propagation vector  $\mathbf{k}$ . Dashed lines on the panels of Figures 3a and 3b correspond to the selection criteria which we have used. Notice that the versus of wave propagation is not terminated through our analysis (for example it cannot distinguish between propagation outwards or inwards with respect to the Sun). However, on the basis of the work of Martin *et al.* (1973), referring to the same streams and the same experimental data considered here, we know (from the sign of the correlation

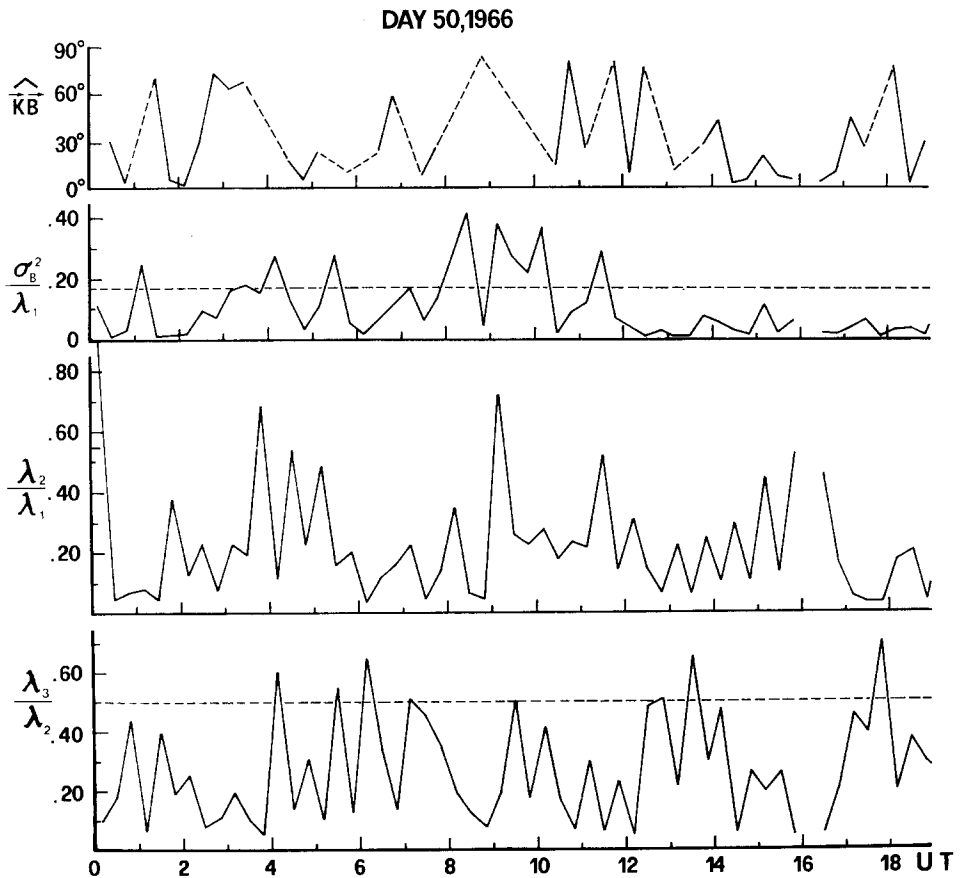


Fig. 3(a).

DAY 52, 1966

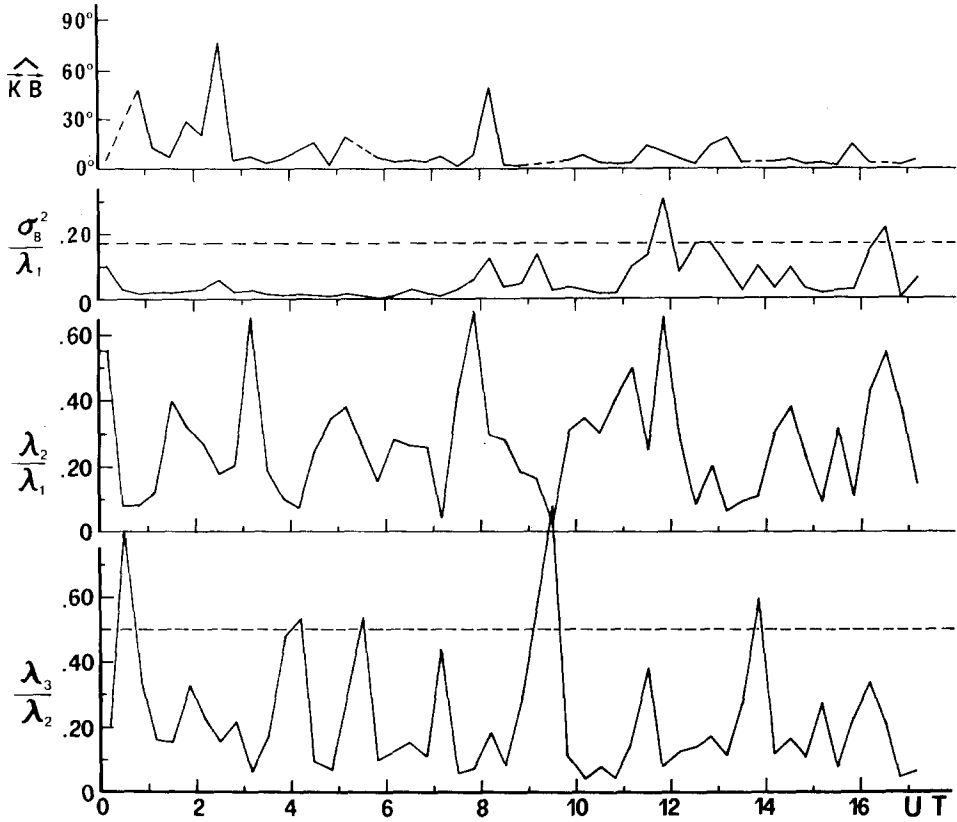


Fig. 3(b).

Fig. 3. From the top are given: the angle between the direction of minimum variance of the magnetic field and the field vector; the ratio of the variance of the field magnitude to the largest eigenvalue of the variance matrix ( $\sigma_B^2/\lambda_1$ ); the ratios of the eigenvalues  $\lambda_2/\lambda_1$  and  $\lambda_3/\lambda_2$ . Each point corresponds to a 20 min interval. (a) of the figure refers to the leading edge of the high velocity stream illustrated in Figure 1; (b) to the trailing edge of the same stream.

between the velocity and magnetic field fluctuations) that the actual direction of propagation is most commonly outwards from the Sun.

**4. General Observational Features of Waves Associated with High Speed Streams**

In this section, prior to a detailed comparison of some of the data with the theory of velocity shear instabilities, we will give a discussion of some general features of the waves which result from the analysis of high speed streams.

The fluctuations of the magnetic field are mainly transversal during all the periods considered in the present analysis: in fact, as seen in the previous section,

only 29 out of 407 blocks have a variance of the field magnitude  $\sigma_B^2 > \lambda_1/6$ . The few cases when  $\sigma_B^2$  exceeded this limit usually occurred inside the compression region at the leading edge of the streams (see Figure 3a). This is consistent with previous observations by Belcher and Davis (1971) who reported that this region may contain significant amounts of non-Alfvénic wave modes. The fact that the compressive components at the leading edge of the streams correspond to magnetosonic modes is however open to question. In Figure 4 we have shown a time history of the magnetic field intensity and the plasma density during a period (Day 50, from 7:00 UT to 10:00 UT) characterized by relatively high values of  $\sigma_B^2$  (see Figure 3a). As it is seen,  $B$  and  $N$  appear to be strongly anti-correlated, which is what one expects, on the basis of simple magnetohydrodynamics in the static case, i.e. for static structures convected by the solar wind. On the contrary, from the theory of small amplitude magnetosonic waves (Stix, 1961), one predicts a positive correlation between fluctuations of  $N$  and  $B$ . On the basis of this we are therefore inclined to conclude (at least for the streams which we have considered), that the leading edges are characterized by compressive static features convected by the wind (besides Alfvén waves, as will be discussed in the following) and less likely by magnetosonic waves.

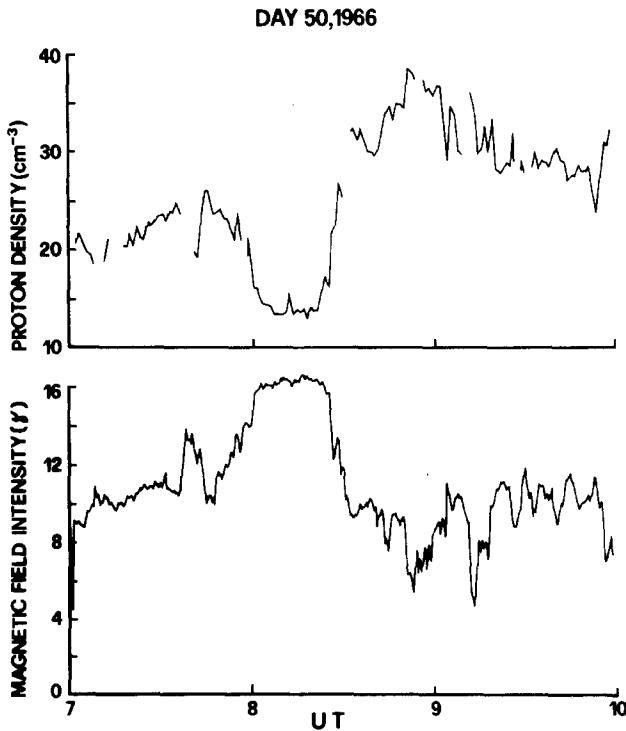


Fig. 4. Interplanetary magnetic field intensity and proton density observed by Pioneer 6 during a 3 hr interval at the leading edge of the high-velocity stream shown in Figure 1.

Figure 5 summarizes the most relevant statistical features of the data considered in the present report. The distribution of the ratio  $\lambda_2/\lambda_1$  (Figure 5a) is strongly peaked between 0.1 and 0.2, with only a few cases at  $\lambda_2/\lambda_1 > 0.5$ . This trend indicates that a quasi-linear polarization of the waves is prevailing. This is quite similar to results given by Chang and Nishida (1973), the different shape of the

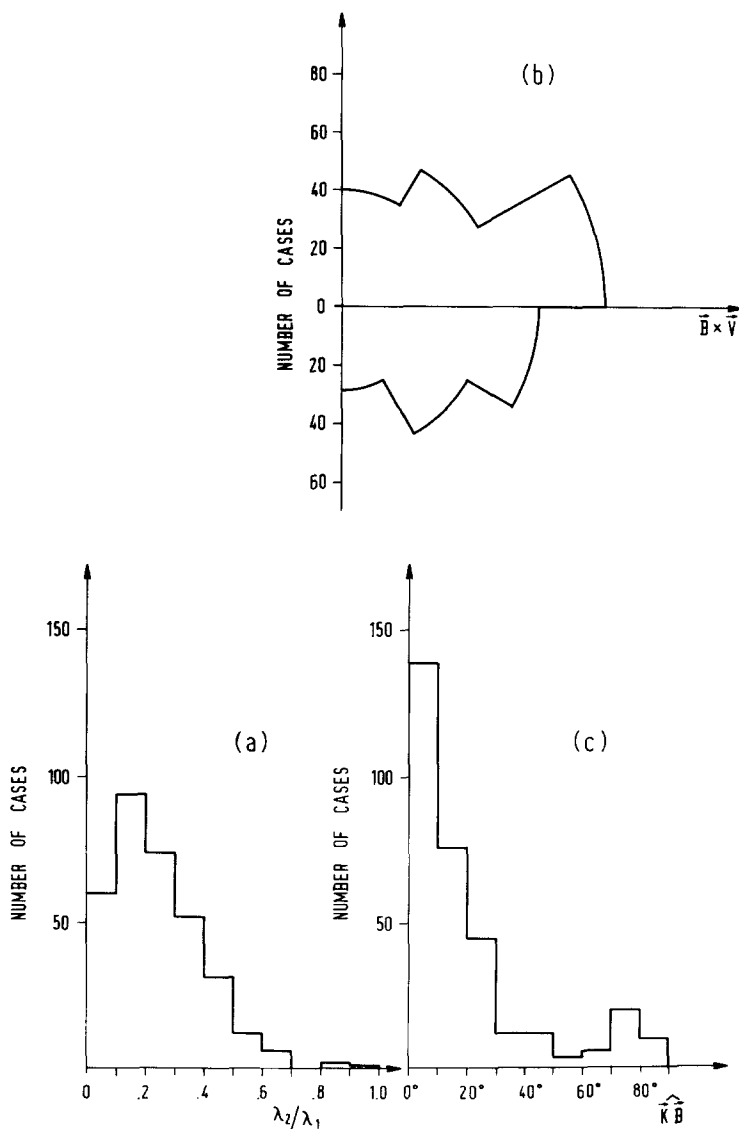


Fig. 5. Statistical distributions of: (a) the ratio between the two largest eigenvalues ( $\lambda_2/\lambda_1$ ) obtained from the minimum variance analysis; (b) the direction of the eigenvector of maximum variance; (c) the angle  $\hat{k} \hat{B}$ , between the eigenvector of minimum variance and the magnetic field. The total number of cases is 331 (each being a 20 min block of data).

$\lambda_2/\lambda_1$  histogram reported by Burlaga and Turner (1976) (showing a significant fraction of circularly polarized waves) is most probably explained by the different methods of analysis adopted (Burlaga and Turner made use of the Daily (1973) filtering technique which we have criticized previously).

The polar histogram in Figure 5b illustrates the direction  $x$  of the eigenvector of maximum variance. In agreement with previous results (e.g. Belcher and Davis, 1971),  $x$  tends to be aligned with the vector  $\mathbf{B} \times \mathbf{r}$  (i.e. with the normal to the ecliptic plane, if  $\mathbf{B}$  is along the Parker's spiral).

Finally, Figure 5c shows the statistical distribution of the angle  $\widehat{\mathbf{kB}}$  ( $\mathbf{k}$  being the direction of minimum variance). The general tendency of  $\mathbf{k}$  to be almost parallel to the magnetic field direction (Belcher and Davis, 1971; Daily, 1973; Chang and Nishida, 1973) is confirmed, even though there is a significant amount of cases in which  $\widehat{\mathbf{kB}}$  is large. A comparison through Figures 3a and 3b, between the leading and trailing portions of the high velocity streams, indicates that the largest values of  $\widehat{\mathbf{kB}}$  occur mainly at the leading edge.

We have investigated in more detail the existence of a relationship between the angle  $\widehat{\mathbf{kB}}$  and the gradient of the solar wind bulk speed ( $V$ ). Figure 6 is a scatter plot of  $\widehat{\mathbf{kB}}$  as a function of the difference between subsequent hourly averages of  $V$ . Positive (negative) values of  $\Delta V$  indicate increases (decreases) of the bulk velocity. It is seen that when  $\Delta V \leq 0$ ,  $\widehat{\mathbf{kB}}$  exceeds  $30^\circ$  during only 10, out of 165, 20 min intervals (6% of cases), while, when  $\Delta V > 0$ ,  $\widehat{\mathbf{kB}} > 30^\circ$  in 53, out of 166 cases (32%). The interpretation is that one has probably Alfvén (almost incompressible)

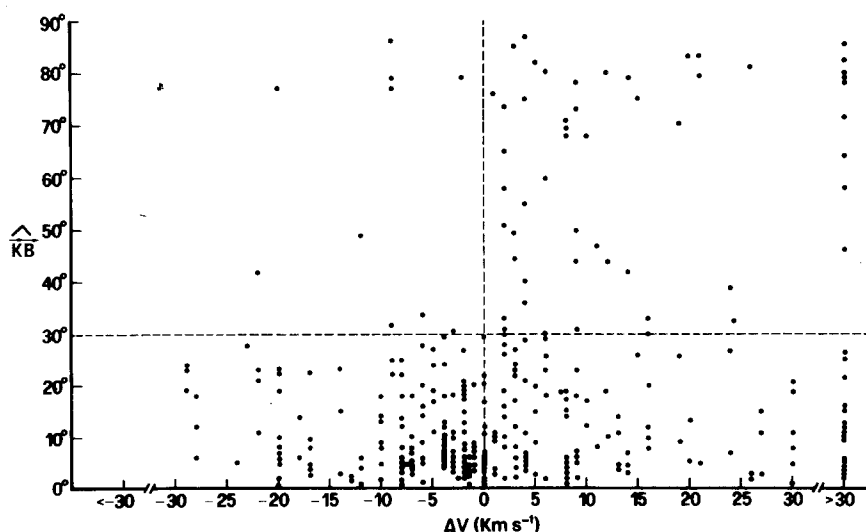


Fig. 6. Scatter plot of  $\widehat{\mathbf{kB}}$  (the angle between the direction of minimum variance of magnetic field and the field vector) as a function of the difference between subsequent hourly averages of the plasma bulk velocity. Each point refers to a 20 min time interval. The broken lines are intended to guide the eye.

waves all along the streams, i.e. both in their leading and in their trailing edges, but whenever the velocity increases (and therefore mainly in the leading edge, but also on limited periods along the trailing edge) such waves are strongly scattered from the direction almost parallel to  $\mathbf{B}$ .

We recall that a scattering or refraction of this type has been predicted by Hollweg (1975) in the framework of a simplified model of a high velocity stream. More precisely, using a triangular velocity profile, Hollweg finds that the direction of  $\mathbf{k}$  should deviate from the direction of  $\mathbf{B}$  in the rising portion of the stream. However the wave direction predicted by this theory cannot be easily compared with the data owing to the oversimplification of the theoretical model (in particular, the theory models the whole stream).

We can still say, however, that the trend shown by Figure 5 may be due to the same effect considered in Hollweg's paper.

### 5. Evidence for Velocity Shear Instabilities in High Speed Streams

The point of view, from now on, is that of selecting periods of time where one has clearly Alfvén waves ( $\sigma_B^2/\lambda_1 \ll 1$ ) with directions of propagation almost parallel to  $\mathbf{B}$ , and compare the plasma, magnetic field and wave data relative to these periods with the theoretical predictions of velocity shear instabilities which have been recalled in Section 2. In turn the selection of the appropriate periods is based on the results of the variance analysis (shown for two days in Figures 3a and 3b). In particular these must be periods with scarce variation of the direction of minimum variance (top panels of Figures 3a and 3b) and very small values of  $\sigma_B^2/\lambda_1$ .

The selected periods are listed in the first two columns of Table I. These are all within trailing edges of the corresponding streams, with the exception of the period from 22:00 UT to 1:00 UT between days 50 and 51, which refers to a compression region. The remainder of the table contains the numerical values of several parameters obtained from the plasma and magnetic field data. More specifically  $\bar{N}$ ,  $\bar{V}$ ,  $\bar{B}$ ,  $\bar{W}$  are averages (in each period) of plasma density, velocity, magnetic field and ion most probable thermal speed, required to calculate average values of the ion cyclotron frequencies and of  $\beta_i$ .  $\Delta V$ ,  $\Delta N$ ,  $\Delta L$  represent velocity and density variations and corresponding scale lengths again for each period. Other two parameters listed in the table are the angle between the wave vector and the average direction of  $\mathbf{B}$ , and the parameter  $\eta$  defined by (15) which enters the formulas for instability of almost parallel Alfvén waves (14).

Notice that the dispersion relations (7), (11), and (14) of Section 2, all exhibit two branches, an unstable and a damped branch. The conditions (10), (12), and (16) which have been called instability conditions, are really the conditions to be satisfied in order to have an imaginary part of the frequency, which has then the two possible signs corresponding to growth and damping. The discussion to follow refers to the possible unstable branches with the obvious understanding that the damped branches will not give any observable wave of a significant level.

TABLE I  
Parameters obtained for six selected periods

Day	Hour	$\bar{N}$ ( $\text{cm}^{-3}$ )	$\bar{V}$ ( $\text{km s}^{-1}$ )	$\bar{B}$ ( $\gamma$ )	$\bar{W}$ ( $\text{km s}^{-1}$ )	$\Delta V$ ( $\text{km s}^{-1}$ )	$\Delta N$ ( $\text{cm}^{-3}$ )	$\Delta L$ (km)	$\widehat{Bn}$	$\eta$	$\lambda_1$ (km)
52	5-8	1.25	590	3.3	50	-37	0.1	$6.37 \times 10^6$	$7^\circ$	$9 \times 10^{-5}$	$1.13 \times 10^6$
52	12-15	1.80	527	4.5	66	-6	0.4	$5.69 \times 10^6$	$7^\circ$	$2 \times 10^{-5}$	$4.92 \times 10^5$
51	21-24	1.10	635	3.2	61	-51	0.2	$6.84 \times 10^6$	$10^\circ$	$1.2 \times 10^{-5}$	$1.17 \times 10^6$
50-51	22-1	5.25	660	9.4	84	+47	1.3	$7.12 \times 10^6$	$9^\circ$	$4 \times 10^{-5}$	$9.13 \times 10^5$
35	14-17	3.8	571	5.1	59	-20	0.9	$6.17 \times 10^6$	$3^\circ$	$1.3 \times 10^{-4}$	$1.01 \times 10^6$
35-36	23-2	3.6	507	6.2	55	-21	0.4	$5.48 \times 10^6$	$14^\circ$	$1.5 \times 10^{-5}$	$4.3 \times 10^5$



Testing of the stability criterion (16) ( $\eta > 0$ ), would require the determination of the sign of  $k_{\parallel}/k_{\perp}$ . This is in principle possible within the minimum variance analysis which has been performed. In practice this information is however not reliable as  $\tan^{-1}(k_{\parallel}/k_{\perp})$  is too small compared with the measurement precision.

The absolute values of  $\eta$  obtained, suposing that (16) is satisfied, allow however, a determination of the growth rate from the relation (14). For  $\eta \ll 1$ , Equation (14) gives for the growth rate  $\gamma$  (which still depends on the parallel wave number  $k_{\parallel}$ ),

$$\frac{\gamma}{k_{\parallel}v_A} \sim \sqrt{\frac{\eta}{2}}. \tag{18}$$

A condition which must be imposed to this instability (or to any other instability) to be of relevance at 1 AU, is that the time for growth of the waves must be much shorter than the convection time  $\tau_{SW}$  of the solar wind plasma from the Sun to 1 AU ( $\tau_{SW} = 4$  days), i.e.

$$\gamma\tau_{SW} \geq 1. \tag{19}$$

Notice that, in (18) the parallel wave number  $k_{\parallel}$  and the angle that the wave direction makes with the average field or, equivalently, the value of  $k_{\parallel}/k_{\perp}$  are two independent parameters. Consequently, there are in principle two ways of interpreting (and testing with the data) condition (19). The first one would be that of referring to waves of a given parallel wavelength  $1/k_{\parallel}$ . In that case (19) would turn into a condition of the type  $\eta > \eta_{\min}$ . According to the definition (15) of  $\eta$ , this leads, in terms of angle of the wave with the magnetic field direction, to a condition  $\alpha < \alpha_{\max}$ , where  $\alpha_{\max} \sim v'_0$ . Hence, in the trailing edge of the streams, where the velocity shear is smaller than in the leading edges, one would predict smaller angles with respect to the magnetic field direction than in the compression regions, in agreement with the observations (see Section 4). However, the conclusion holds for a fixed  $k_{\parallel}$ , whereas in the data we see the combined effect of a spectrum of waves, i.e. an entire range of  $k_{\parallel}$  values. Notice also that (for the actual values of  $v'_0$  and  $\Omega_{ci}$ )  $\alpha_{\max}$  is very small. The much larger angles which are experimentally observed in the leading edges of the streams are more likely due to the diffraction effects (Hollweg, 1975) mentioned in Section 4.

A second way of using condition (19), is that of taking the angle  $\alpha$  (or the value of  $k_{\parallel}/k_{\perp}$ ) from the data and then derive from (19) a condition on the parallel wavelength of the excited waves. In this case we obtain a lower limit for the parallel wavelength,

$$\lambda_{\parallel} \ll \lambda_1 \equiv 2\pi\sqrt{\frac{\eta}{2}}(v_A\tau_{SW}) \tag{20}$$

which can be computed from the results of the previous data analysis. The next point is to decide if the spectrum of observed wavelengths fall into the range defined by condition (20). The values obtained for  $\lambda_1$ , listed in the last column of Table I, are in the range  $5 \times 10^5 - 1 \times 10^6$  km.

Notice that such values are of the same order of magnitude as the longest wavelengths which can be investigated through our variance analysis based on 20 min periods.

Looking at the magnetic data for the periods considered, we can clearly see fluctuations on time scales down to about 1 min, which correspond (looking at the velocity values listed in Table I) to wavelengths

$$\lambda_{\min}^{\text{observ.}} \sim (1.5-2) \times 10^4 \text{ km.} \quad (21)$$

We recall that Alfvénic fluctuations on time scales as short as 30 s, have been evidenced in the analysis of Martin *et al.* (1973), based on Pioneer 6 data and embracing also the periods considered here.

The conclusion is therefore that the wavelengths of the unstable Alfvén waves, as calculated from theory using all the measured parameters (using (20)), are within the range of the observed wavelengths.

This is a proof of consistency of the data (showing almost parallel Alfvén waves) with the theory of local generation of the waves through a velocity shear instability, although it is not a definite proof that such instability causes the waves, as we have not checked the instability criterion (16).

Having checked condition (20), it should now be recalled that the spectrum of the Alfvén waves, in the solar wind (Belcher and Davis, 1971; Burlaga and Turner, 1977) includes actually wavelengths above the limit  $\lambda_1$  (defined in (20)), (and above the limit set up by our choice of 20 min periods) and, in fact, ranging up to  $5 \times 10^6$  km.

One of our conclusions is therefore that, if velocity shear instabilities are playing a role, they will tend to generate waves in the higher frequency (or shorter wavelength) part of the spectrum.

Other mechanisms (and most likely generation at the Sun), and not velocity shear instabilities, are responsible for the longer wavelength part of the Alfvén wave spectrum. It is furthermore plausible that even part of the waves of shorter wavelengths, in the range (20), are of solar origin: our positive check of condition (20) simply indicates that the wave excitation by velocity shear should also be relevant in that part of the spectrum.

The theory recalled in Section 2 predicts also the possibility of almost perpendicular waves (both magnetosonic and Alfvénic) driven by velocity shear, but such waves are not observed (see Figure 3). Thus, it is necessary to check whether these types of waves should arise, according to the theory, for the actual values of the plasma and magnetic field parameters.

The type of comparison we have done is the following: for both types of quasi-perpendicular waves, by looking at the corresponding instability criteria (10) and (12) we can find the value of  $k_{\perp}/k_{\parallel}$  which minimizes such criteria (written in the form  $F(k_{\perp}/k_{\parallel}) > 0$ ): from this value a minimum velocity shear necessary to excite the instability can be derived. For quasi-perpendicular Alfvén and magnetosonic

waves it is found respectively:

$$\left(\frac{\Delta V}{\Delta L}\right)_{\perp, A} = \frac{1}{2}(1 + \beta)\beta_i^{1/2} \frac{V_{thi}}{L_N}, \tag{22}$$

$$\left(\frac{\Delta V}{\Delta L}\right)_{\perp, MS} = (1 + \beta)^{1/2} \left(1 + \frac{T_e}{T_i}\right)^{1/2} \frac{V_{thi}}{L_N}. \tag{23}$$

In Table II we have reported, corresponding to the same periods considered in Table I, the threshold values obtained from (22) and (23) together with the observed values of  $\Delta V/\Delta L$ . It is seen that in some cases the threshold values are above the observed values. There are also cases, however, where  $(\Delta V/\Delta L)_{observ.}$  is slightly greater than one or both the above thresholds. These cases are close to marginal stability and we must expect very small growth rates. A computation of such growth rates, in terms of  $k_{\perp}$  (of which we do not report any detail) and subsequent application of the convection criterion (19) gives upper limits for the perpendicular wavelengths which could be observed, which are extremely small ( $\sim 50\text{--}100$  km) in comparison with the minimum wavelengths observed given by (21). This means that, for the parameters corresponding to the periods considered, no quasi perpendicular waves can be excited by velocity shear, consistent with the data showing only almost parallel waves. We also have that possible evidence of quasi-perpendicular velocity shear instabilities, with velocity gradients of the type measured, could only be searched at much smaller wavelengths and therefore with much higher resolution data.

TABLE II  
Computed (from (22) and (23)) and observed  $\Delta V/\Delta L$  values

Day	Hour	$L_N$ (km)	$\beta_i$	$\beta$	$\left(\frac{\Delta V}{\Delta L}\right)_{\perp, A}$ (s <sup>-1</sup> )	$\left(\frac{\Delta V}{\Delta L}\right)_{MS}$ (s <sup>-1</sup> )	$\left(\frac{\Delta V}{\Delta L}\right)_{observ.}$ (s <sup>-1</sup> )
52	5-8	$7.9 \times 10^7$	0.61	1.22	$5.4 \times 10^{-7}$	$1.3 \times 10^{-6}$	$5.8 \times 10^{-6}$
52	12-15	$2.5 \times 10^7$	0.82	1.64	$3.1 \times 10^{-6}$	$5.9 \times 10^{-6}$	$1.1 \times 10^{-6}$
51	21-24	$3.7 \times 10^7$	0.85	1.70	$2.0 \times 10^{-6}$	$3.8 \times 10^{-6}$	$7.4 \times 10^{-6}$
50-51	22-1	$2.8 \times 10^7$	0.89	1.78	$3.8 \times 10^{-6}$	$6.9 \times 10^{-6}$	$6.6 \times 10^{-6}$
35	14-17	$2.6 \times 10^7$	1.05	2.10	$3.6 \times 10^{-6}$	$5.6 \times 10^{-6}$	$3.2 \times 10^{-6}$
35-36	23-2	$4.9 \times 10^7$	0.58	1.17	$9.3 \times 10^{-7}$	$2.3 \times 10^{-6}$	$3.8 \times 10^{-6}$

### 6. Conclusion and Discussion

We summarize here what has been obtained and discuss its actual relevance.

We have tested our data analysis on two high velocity streams against theories of wave generation through velocity shear instabilities.

In all periods where Alfvén waves were clearly observed, with propagation vector almost parallel to **B**, we found that the wavelengths observed through our

minimum variance analysis (from  $\sim 2 \times 10^4$  to  $\sim 5 \times 10^5$  km) fall within the wavelength range which is predicted (see condition (20)) from application of a theory of wave generation through velocity shear.

This is the degree of evidence we give of the possible role of such instabilities. We suggest correspondingly that velocity shear instabilities may be a relevant mechanism to generate Alfvén waves in the short wavelength part of the spectrum. Alfvén waves of wavelengths larger than the value  $\lambda_1$ , given in (20), are certainly not due to such instabilities and, most likely, have been generated at the Sun photosphere. On the other hand, in the short wavelength range (20) both waves generated at the Sun and waves due to a velocity shear instability could be present.

It should be remarked that the linear stability theory which we have applied for Alfvén wave generation, does not give a preferential direction of propagation for the excited waves. The criterion (16), for a given sign of  $v'_0$ , is in fact a requirement on the sign of  $k_{\parallel}/k_{\perp}$  (and not of  $k_{\parallel}$ ). This in contrast with a general feature of Alfvén waves, reported in the literature, namely that their propagation is generally outwards from the Sun. However, it should be recalled that we are not excluding, in the shorter wavelength range (20), waves of solar origin, but simply point out the possibility of having also waves of more local origin driven by velocity shear. Waves of solar origin, if also present, would on the other hand again give a general indication of outward propagation.\*

Observed spectra of the interplanetary magnetic field are of the type  $f^{-\alpha}$  ( $\alpha \sim 1.5-2.2$ ) and hence show decreasing power with increasing frequency. On the other hand, the instability of Alfvén waves driven by velocity shear has a growth rate increasing for shorter wavelengths. The contradiction is however only apparent. In the wavelength range (20) waves arising from velocity shear instability are most probably mixed to waves having different origins and even to other non-Alfvénic fluctuations (such as discontinuities). The power spectra of the interplanetary magnetic field, depending from all these fluctuations, will not therefore reflect only the features of the waves driven by velocity shear.

Concerning the polarization of the observed Alfvén waves (see Section 4), we remark that the instability theory which we have applied, being a linear theory, cannot predict polarization properties of the large amplitude waves. Discussions on the possible causes of the observed polarization have been given by Belcher and Davis (1971) and Hollweg (1975).

Finally we have tested that the plasma and magnetic field parameters, in particular the local velocity gradients, for the periods analyzed, if compared with theory of generation of quasi-perpendicular magnetosonic and Alfvén waves, again through velocity shear, imply that waves of wavelength in the observed range cannot be excited. Thus, this comparison gives further consistency with the observations which show no evidence of quasi-perpendicular waves.

\* Note that this conclusion is obtained using plasma and magnetic field data averaged over  $\sim 5$  min periods (Belcher and Davis, 1971).

In conclusion, we should say that, in order to explore in more detail the relevance of the idea of Alfvén wave generation through the velocity shear instability we have been considering, it is very important to consider data at higher resolution than the one used here, as for example the magnetic data of the HELIOS spacecraft. This would lead to a more satisfactory definition of wave properties in the region of higher frequencies, where, according to this investigation, the contribution of waves driven by velocity shear should be relevant.

### Acknowledgements

Plasma data from the Pioneer 6 experiment were kindly supplied by Dr A. Lazarus of the Massachusetts Institute of Technology.

Magnetic field data were made available by Dr N. Ness of the Goddard Space Flight Center (Washington). This research has been supported by the Consiglio Nazionale delle Ricerche of Italy.

### References

- Abraham-Shranner, B. and Feldman, W. C.: 1977, *J. Geophys. Res.* **82**, 618.  
 Barnes, A. and Hollweg, J. V.: 1974, *J. Geophys. Res.* **79**, 2302.  
 Belcher, J. W. and Davis, L. Jr.: 1971, *J. Geophys. Res.* **76**, 3534.  
 Belcher, J. W., Davis, L. Jr., and Smith, E. J.: 1969, *J. Geophys. Res.* **74**, 2302.  
 Burlaga, L. F. and Turner, J. M.: 1976, *J. Geophys. Res.* **81**, 73.  
 Chandrasekhar, S.: 1961, *Hydrodynamic and Hydromagnetic Stability*, Oxford University Press, London, Chapter 11, p. 481.  
 Chang, S. D. and Nishida, A.: 1973, *Astrophys. Space Sci.* **23**, 301.  
 Daily, W. D.: 1973, *J. Geophys. Res.* **78**, 2043.  
 Dobrowolny, M.: 1972, *Phys. Fluid* **15**, 2263.  
 Dobrowolny, M.: 1977, *Phys. Fluid* **20**, 1027.  
 Dobrowolny, M. and Paravano, A.: 1977, *Il Nuovo Cimento B*, in press.  
 Feldman, W. C., Asbridge, J. R., Bame, S. J., and Montgomery, M. D.: 1974, *Rev. Geophys. Space Phys.* **12**, 715.  
 Gary, S. P., Feldman, W. C., Forslund, D. W., and Montgomery, M. D.: 1975, *J. Geophys. Res.* **80**, 4197.  
 Hollweg, J. V.: 1973, *Astrophys. J.* **181**, 547.  
 Hollweg, J. V.: 1975, *Rev. Geophys. Space Phys.* **13**, 263.  
 Hollweg, J. V.: 1975, *J. Geophys. Res.* **80**, 908.  
 Jenkins, G. M. and Watts, D. G.: 1969, *Spectral Analysis and its Applications*, Holden-Day, San Francisco, California.  
 Kadomtsev, B. B.: 1965, *Plasma Turbulence*, Academic Press, New York, p. 78.  
 Lazarus, A. J., Heinemann, M. A., McKinnins, R. W., and Bridge, H. S.: 1973, 'Solar Wind Data from the MIT Plasma Experiments on Pioneer 6 and Pioneer 7', NASA, NSSDC 73-08.  
 Martin, R. N., Belcher, J. W., and Lazarus, A. J.: 1973, *J. Geophys. Res.* **78**, 3653.  
 Ness, N. F.: 1970, *Space Sci. Rev.* **11**, 459.  
 Ness, N. F., Scarce, C. S., and Cantarano, S.: 1966, *J. Geophys. Res.* **71**, 3305.  
 Stix, T. H.: 1962, *The Theory of Plasma Waves*, McGraw-Hill Book Co.